Kinetic and Thermodynamic Evidence for Flipping of a Methyl-CpG Binding Domain on Methylated DNA†

Kosuke Inomata,‡ Izuru Ohki,§ Hidehito Tochio,*,‡ Kenichiro Fujiwara,|| Hidekazu Hiroaki,⊥ and Masahiro Shirakawa*,‡,#

Department of Molecular Engineering, Graduate School of Engineering, Kyoto University, Katsura, Kyoto 615-8510, Japan, CREST, Japan Science and Technology Corporation, 4-1-8, Honcho, Kawaguchi, Saitama 332-0012, Japan, Division of Structural Biology, Medical Institute of Bioregulation, Kyushu University, 3-1-1 Maidashi, Higashi-ku, Fukuoka 812-8582, Japan, Field of Supramolecular Biology, International Graduate School of Arts and Sciences, Yokohama City University, 1-7-29, Tsurumi, Yokohama, Kanagawa 230-0045, Japan, and Division of Structural Biology, Graduate School of Medicine, Kobe University, 7-5-1, Kusunoki-cho, Chuo-ku, Kobe, Hyogo 650-0017, Japan

Received September 17, 2007; Revised Manuscript Received December 19, 2007

ABSTRACT: The methyl-CpG binding domain (MBD) is a conserved domain in transcriptional factors that binds to methylated CpG dinucleotide DNA sequences in vertebrates. The complex is comprised of an asymmetric MBD monomer and a symmetric DNA duplex. Therefore, in the complex, each strand of the duplex DNA is in contact with the protein at a distinct surface and thus exhibits a different chemical shift in NMR spectra. Two-dimensional chemical exchange spectroscopy revealed the presence of a stochastic exchange of the two strands of the duplex DNA in the complex at a rate of 4 s^{-1} at 25 °C, which indicates the existence of a motion of the MBD such that the orientation of the MBD becomes reversed with respect to the DNA duplex. Kinetic and thermodynamic analyses using surface plasmon resonance, quartz crystal microbalance, and isothermal titration calorimetry suggest that the reversal of MBD with respect to the DNA duplex takes place without its complete dissociation from DNA, indicating the presence of an intermediate protein−DNA binding state that allows the protein to undergo a flip motion upon DNA.

DNA methylation in mammalian cells occurs at the 5-position of cytosine within the CpG sequence (*1*) and is important for control of gene activity either through effects on a single promoter region or through global mechanisms that affect many genes (*2*–*4*). DNA methylation often exerts its function through its recognition by proteins that contain conserved methyl-CpG binding domains (MBDs)[1] (*5*). We have previously determined the solution structure of the MBD from human MBD1 [residues 1–75, designated as $MBD1_{(1–75)}$] in complex with methylated DNA by NMR (*6*). $MBD1_{(1–75)}$ binds to a duplex DNA that contains the symmetric methyl-CpG sequence, and the binding is independent of the DNA sequences flanking the site (*5*–*7*). DThis property makes $MBD1_{(1–75)}$ unique among sequence-specific DNA binding proteins, as an asymmetric monomer $MBD1_{(1–75)}$ can bind to a symmetric DNA motif. For the structure determination of the MBD−DNA complex, we used a 12 bp palindromic DNA duplex containing a methyl-CpG sequence at its center, to avoid the generation of nonequivalent complexes. In the complex, each strand of the DNA duplex interacts with $MBD1_{(1–75)}$ at a distinct surface, although the nucleotide sequences of the strands are identical. This was indicated by the observation that chemical shifts of sugar and base protons of one strand differ from those of the other strand in the complex (Figure 1), while the same shifts are completely degenerate when the DNA duplex is free from $MBD1_{(1–75)}$.

In the structural studies of the $MBD1_{(1–75)}$–DNA complex, we measured two-dimensional (2D) $^1H-^1H$ NOESY spectra of the DNA in the complex and found a number of interstrand cross-peaks which did not likely originate from dipole–dipole interactions but by a chemical exchange process. This observation indicates that there is a motion of $MBD1_{(1–75)}$ such that the orientation becomes reversed with respect to the DNA duplex on the NMR time scale (an order of milliseconds). Such an exchange phenomenon was previ-

† This work was supported by grants to M.S. and H.T. from the Japanese Ministry of Education, Science, Sports and Culture and to M.S. from Core Research for Evolution Science and Technology (CREST) of the Japan Science and Technology Agency. This research was also supported in part by the Global COE Program "International Center for Integrated Research and Advanced Education in Materials Science" (B-09) of the Ministry of Education, Culture, Sports, Science and Technology (MEXT) of Japan, administrated by the Japan Society for the Promotion of Science. We acknowledge support by the Global COE Program "Integrated Materials Science" (B-09)

* To whom correspondence should be addressed. H.T.: Department of Molecular Engineering, Graduate School of Engineering, Kyoto University, Nishikyo-Ku, Kyoto 615-8510, Japan; phone, +81-75-383-2536; fax, +81-75-383-2541; e-mail, tochio@moleng.kyoto-u.ac.jp. M.S.: Department of Molecular Engineering, Graduate School of Engineering, Kyoto University, Nishikyo-Ku, Kyoto 615-8510, Japan; phone, +81-75-383-2535; fax, +81-75-383-2541; e-mail, shirakawa@moleng.kyoto-u.ac.jp.

‡ Kyoto University.

§ Kyushu University.

|| Yokohama City University.

⊥ Kobe University.

Japan Science and Technology Corp.

[1] Abbreviations: MBD, methyl-CpG binding domain; SPR, surface plasmon resonance; QCM, quartz crystal microbalance; ITC, isothermal titration calorimetry.

10.1021/bi7019029 CCC: $40.75
Published on Web 02/12/2008

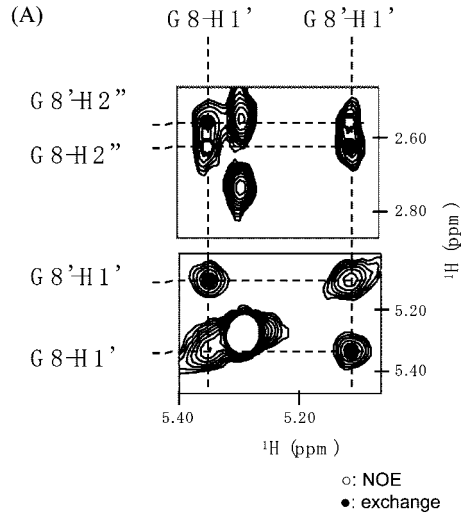

FIGURE 1: Selected regions of the two-dimensional (ω_1)-^{13}C-filtered-(ω_2)-^{13}C-filtered NOESY spectrum of the complex of the methylated DNA and doubly ^{13}C- and ^{15}N-labeled MBD1$_{(1–75)}$. The chemical shifts of G8 H1′ and G8′ H1′ protons of the DNA are indicated. The spectrum was measured on a sample containing 20 mM potassium phosphate (pH 6.5), 50 mM KCl, 5 mM DTT, and 0.5 mM protein−DNA complex at 25 °C. The NOESY mixing time was 300 ms. The internuclear distance between the G8 H1′ and G8′ H1′ protons is 10 Å in the determined structure of the complex of the methylated DNA and MBD1$_{(1–75)}$ (PDB entry 1IG4). (B) Sequence of the olignucleotide used in this study. The mC bases are methylated at the 5-positions.

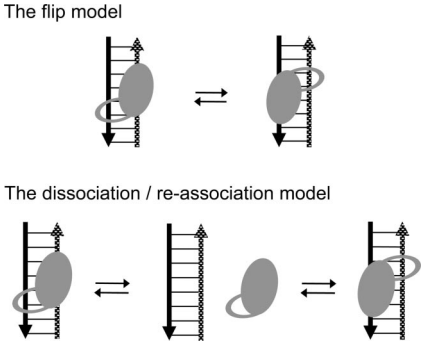

FIGURE 2: Schematic representation of the two possible models to explain the DNA strand exchange. The flip model (top) in which the protein reverses its orientation without total dissociation from the DNA. The dissociation−reassociation model (bottom) in which the protein is completely detached from the DNA and rebinds to DNA in a random orientation.

ously reported for a protein−drug complex, i.e., HIV protease/inhibitor (*8*), although, to our knowledge, it has not been reported for complexes between biomacromolecules, such as protein−protein or protein−DNA complexes.

Either of the following two models can account for this exchange phenomenon: the flip model (Figure 2, top) in which the protein reverses its orientation without total dissociation from the DNA and the dissociation−reassociation model (Figure 2, bottom) in which the protein is completely detached from the DNA stochastically and rebinds to DNA in a random orientation (Figure 2). The key difference between the two models is whether complete dissociation of the protein from the DNA is necessary for the reversal of the bound protein. To address this question, it is essential to compare the rates of both the reversal of the MBD1$_{(1–75)}$ orientation in the MBD1$_{(1–75)}$−DNA complex and the dissociation of the complex. For this purpose, we performed kinetic and thermodynamic studies of the complex using NMR, surface plasmon resonance (SPR), quartz crystal microbalance (QCM), and isothermal titration calorimetry (ITC). The results indicate that the rate of the flipping was much greater than the dissociation rate and thus supports the flip model, suggesting the existence of a transient binding state that might be related to a nonspecific MBD1$_{(1–75)}$−DNA complex.

MATERIALS AND METHODS

Sample Preparation. The doubly ^{15}N- and ^{13}C-labeled MBD1 MBD [MBD1$_{(1–75)}$] was expressed in *Escherichia coli* strain BL21(DE3) as a glutathione *S*-transferase (GST) fusion protein. For ^{15}N and ^{13}C double labeling, the bacteria were grown in synthetic media which contained $^{15}NH_4Cl$ and [^{13}C]glucose as the sole nitrogen and carbon sources, respectively. The fusion protein was purified as previously reported (*6, 9*). The palindromic 12-mer (5′-GTATCCG-GATAC-3′) and biotin-tagged 20-mer (5′-Bio-AAAAAA-GATCGACGACGTAC-3′, Bio = biotin) and 14-mer (5′-GATCGACGACGTAC-3′) oligonucleotides, in which the underlined cytosine (C) base was either methylated or not, were purchased from Hokkaido System Science (Sapporo, Japan). The oligonucleotides were annealed to form the self-complementary duplex DNA. The MBD1$_{(1–75)}$−DNA complex for NMR experiments was formed by titrating the DNA solution into the protein solution. To achieve 1:1 stoichiometry, the amide ^{1}H−^{15}N resonances of the protein were monitored during the titration. All the experiments were performed in buffer containing 20 mM potassium phosphate buffer (pH 6.5), 5 mM DTT, and 50 mM KCl.

NMR Spectroscopy. NMR experiments were performed at 15−30 °C on a Bruker DRX500 spectrometer equipped with a cryogenic triple-resonance probe head. The samples were prepared in 250 μL H_2O/D_2O solutions (90%/10%) containing 20 mM potassium phosphate buffer (pH 6.5). Two-dimensional F_1, F_2 ^{13}C-filtered NOESY spectra (*10*) of the doubly ^{13}C- and ^{15}N-labeled MBD$_{(1–75)}$−methylated DNA complex (0.5 mM) with mixing times of 30, 60, 120, 200, and 300 ms were recorded. Of them, those with mixing times of 200 and 300 ms were not used for the analysis, as these data did not satisfy the criteria proposed by Katoh et al. (*8*), because of apparent spin diffusion or relaxation effects. Each spectrum was acquired for ∼16 h. The matrix size was 256 (t_1) × 1024 (t_2) with spectral widths of 8013 Hz (F_1) and 5682 Hz (F_2), respectively. All NMR spectra were processed and analyzed with NMRPipe (*11*) and Sparky (*12*). The heights of the cross-peaks and diagonal peaks were used as peak intensities to obtain the buildup curve (Figure 3A). The buildup curves were fitted to eq 1 to estimate k_{ex} values using Origin (Microcal).

Surface Plasmon Resonance (SPR) Analyses. The dissociation and association rates and the dissociation constant for MBD1$_{(1–75)}$ and the oligonucleotide DNAs were analyzed by using a BIAcoreX or BIAcore3000 instrument (GE Healthcare). Streptavidin-coated SA sensor chips (GE Health-

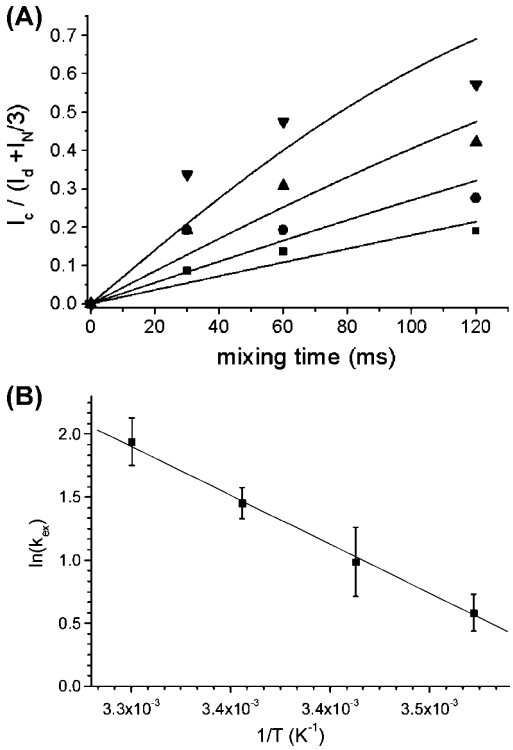

FIGURE 3: Cross-peak buildup curves and Arrhenius plot. (A) The ratios of cross-peak intensities $[I_c/(I_d + I_N/3)]$ are plotted for G8 H1′ and G8′ H1′ as a function of NOESY mixing time at different temperatures [15 (■), 20 (●), 25 (▲), and 30 °C (▼)]. The best fit curves to the experimental data using eq 1 (see the text) are also shown. Obtained k_{ex} values are 1.81 ± 0.26, 2.78 ± 0.69, 4.30 ± 0.51, and 7.08 ± 1.29 s^{-1} at 15, 20, 25, and 30 °C, respectively. (B) Arrhenius plot of ln(k_{ex}) vs 1/T for the G8 H1′−G8′ H1′ cross peak. The best fit line to the data using eq 2 is also shown. Errors were estimated from fitting errors in k_{ex} by employing a Monte Carlo simulation.

care) were used for all experiments. Five microliters of biotin-attached, methylated, or nonmethylated DNA 20-mer (20 μg/mL) was immobilized in buffer containing 20 mM potassium phosphate (pH 6.5), 50 mM KCl, and 5 mM DTT. During the immobilization step, typically SPR responses with response units (RU) of approximately 600 were observed. The binding of $MBD1_{(1–75)}$ to the DNAs was assessed in the same buffer at a flow rate of 50 μL/min with protein concentrations of 10–100 nM at 25 °C for methylated DNA. For the analysis of the data, BIAevaluation version 3.0 was used. The dissociation and association rates (k_{off} and k_{on}, respectively) of $MBD1_{(1–75)}$ for the methylated DNA were estimated from the global fitting procedure, in which response curves at variable concentrations were simultaneously fitted to a simple 1:1 Langmuir model. The model assumed an independent binding event between monovalent analyte protein and monovalent ligand DNA. The equilibrium dissociation constants (K_D) were calculated from k_{on} and k_{off} ($K_D = k_{off}/k_{on}$).

Quartz Crystal Microbalance (QCM) Analyses. The interaction between $MBD1_{(1–75)}$ and methylated DNA was studied by using a 27 MHz AFFINIX Q quartz crystal microbalance (QCM) detector (Initium, Inc.) (*13*). The biotin-attached methylated 20-mer (6.0 ng) and 14-mer (3.6 ng) DNAs were annealed, and the obtained duplex was immobilized on the QCM gold electrode conjugated with avidin (NeutrAvidin, Pierce, Inc.). The electrode was then immersed in a solution (8 mL) containing 20 mM potassium phosphate (pH 6.5), 50 mM KCl, and 5 mM DTT. The rates of dissociation and association for $MBD1_{(1–75)}$ and DNA were determined from the frequency changes (ΔF) upon injection of a $MBD_{(1–75)}$ solution (2.5−15 nM). The electrode immobilized with nonmethylated DNA showed no significant response upon addition of $MBD1_{(1–75)}$ (data not shown). The experiments were performed at 25 °C.

Isothermal Titration Calorimetry (ITC). A Microcal MCS calorimeter was used for the ITC measurements. All solutions used were carefully degassed prior to the titration experiments. The methylated DNA solution (485 μM) was titrated into 2.3 mL of the protein solution (15 μM). For the first titration step, 2 μL of a DNA solution was injected, followed by a 5 μL injection which was repeated 27 times. The heat that arose from the dilution of the DNA solution was independently measured and was subtracted from those measured for the $MBD_{(1–75)}$−DNA interactions. The data were analyzed by using Origin (Microcal) supplied by the manufacturer.

RESULTS

Determination of the Rate of Reversal of $MBD1_{(1–75)}$ on the DNA. To determine the rate of the reversal of $MBD1_{(1–75)}$, we measured 2D F_1, F_2 ^{13}C-filtered NOESY spectra of the duplex DNA complexed with doubly ^{13}C- and ^{15}N-labeled $MBD1_{(1–75)}$ with a variety of mixing times and analyzed the buildup curves of several exchange cross-peaks. We chose cross-peaks attributed to G8 H1′ and G8′ H1′ because these are well resolved from the others in the spectra (see Figure 1 for G8 H1′ and G8′ H1′). In addition, the proton pairs are separated by more than 10 Å in the determined complex structure (PDB entry 1IG4), and thus, the contribution from direct dipole–dipole interactions (nuclear Overhauser effects) can be neglected. Assuming that these cross-peaks arose solely from the chemical exchange between the strands of DNA, the intensity ratio of the diagonal and cross-peaks is given by

$$I_c/(I_d + I_N/3) = [1 - \exp(-2k_{ex}t)]/[1 + \exp(-2k_{ex}t)] \quad (1)$$

where k_{ex} is the rate of the chemical exchange, I_c and I_N are the intensities of the exchange and NOE cross-peaks, respectively, and I_d is the intensity of the diagonal peaks (*8*). Note that addition of $I_N/3$ to I_d is to correct for the depletion of the diagonal peak by the NOE cross-peaks as previously discussed (*8*). Least-squares fitting of the time dependency of $I_c/(I_d + I_N/3)$ to eq 1 yielded k_{ex} values, 1.81 ± 0.26, 2.78 ± 0.69, 4.30 ± 0.51, and 7.08 ± 1.29 s^{-1} at 15, 20, 25, and 30 °C, respectively (Figure 3A). Then, to estimate the activation energy, E_a, for the exchange process, the k_{ex} values in the temperature range between 15 and 30 °C were fitted to the Arrhenius equation

$$k_{ex} = A \exp(-E_a/RT) \quad (2)$$

where A is a constant and T is the temperature in kelvin. The k_{ex} values at various temperatures are described well by the equation, and the estimated activation energy was 15.1 ± 0.41 kcal/mol (Figure 3B).

Rates of Dissociation and Association for $MBD1_{(1–75)}$ and DNA. Rates of dissociation and association between $MBD1_{(1–75)}$ and DNA were independently measured using

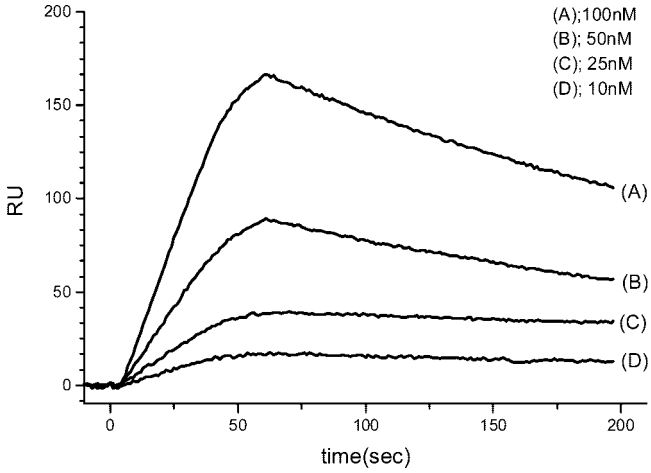

FIGURE 4: Dose−response curves of the surface plasmon resonance (SPR) sensorgram with immobilized methylated DNA for $MBD1_{(1–75)}$. Concentrations of $MBD1_{(1–75)}$ were (A) 100, (B) 50, (C) 25, and (D) 10 nM.

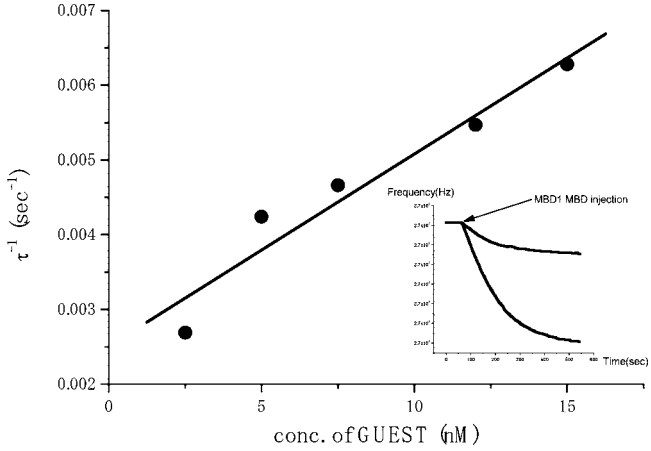

FIGURE 5: Reciprocal plots of relaxation time (τ) obtained from the quartz crystal microbalance (QCM) measurements and the concentration of the guest [$MBD1_{(1–75)}$]. The line indicates the best fit to the data of eq 3 (see the text). The square related coefficient (R^2) is 0.929. The inset shows typical sensorgrams obtained upon $MBD1_{(1–75)}$ injection [7.5 (top) and 15 nM (bottom)].

two different methods, SPR and QCM. The SPR response curves of the DNA-immobilized sensor chips upon application of various concentrations of $MBD_{(1–75)}$ are shown in Figure 4. Response curves obtained at different concentrations were globally fitted to a simple 1:1 Langmuir equation to estimate a single set of k_{off} and k_{on} values. k_{on}, k_{off}, and the dissociation constant, K_D, were estimated to be $(4.63 \pm 0.17) \times 10^4\ M^{-1}\ s^{-1}$, $(3.26 \pm 0.03) \times 10^{-3}\ s^{-1}$, and $(7.04 \pm 0.32) \times 10^{-8}$ M, respectively. The global χ^2 value calculated with BIAevaluation was 4.38 RU, which was comparable to the noise level of sensorgrams, indicating good estimation of the parameters.

A typical QCM sensorgram from the gold sensor chip, onto which was immobilized methylated DNA, upon addition of the $MBD1_{(1–75)}$ is shown in Figure 5, which shows the resonance frequency change associated with the $MBD1_{(1–75)}$−DNA interaction. The k_{on} and k_{off} values are derived from the observed rate constant, defined by τ^{-1}, by application of the following equation (*14*):

$$\tau^{-1} = k_{on}[MBD1_{(1–75)}] + k_{off} \quad (3)$$

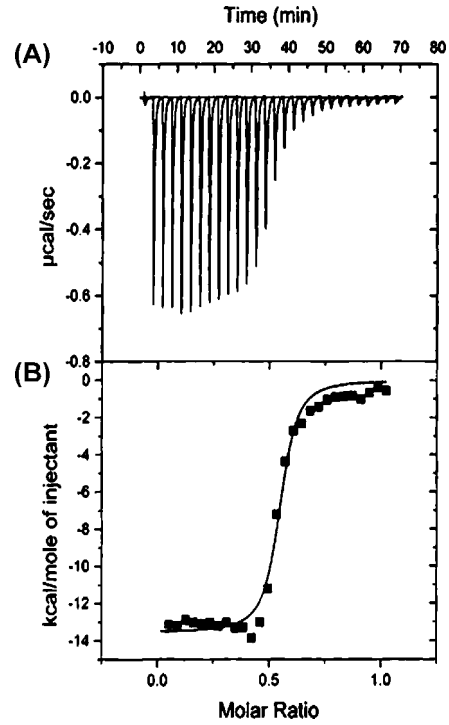

FIGURE 6: Isothermal titration calorimetric (ITC) measurements. (A) An ITC thermogram for binding of $MBD1_{(1–75)}$ to the methylated DNA is shown. Typically, 5 μL each of the protein (485 μM) was titrated into 2.3 mL of the methylated DNA solution (15 μM). (B) Plot of corrected heat values. The line indicates the best fit to the data of a simple 1:1 binding model. The dissociation constant, K_D, and the enthalpy change, ΔH, were $(47.5 \pm 8.7) \times 10^{-9}$ M and -13.5 ± 0.87 kcal/mol, respectively.

k_{on}, k_{off}, and the dissociation constant, K_D, are estimated to be $(2.57 \pm 0.39) \times 10^5\ M^{-1}\ s^{-1}$, $(2.51 \pm 0.38) \times 10^{-3}\ s^{-1}$, and $(9.77 \pm 2.96) \times 10^{-9}$ M, respectively.

Isothermal Titration Calorimetry (ITC) Measurements. ITC was used to analyze the affinity of $MBD1_{(1–75)}$ for the methylated DNA and the thermodynamic properties of the interaction. An exothermic heat pulse was observed after each injection of $MBD1_{(1–75)}$ into the DNA solution at 25 °C (Figure 6A). The area of each exothermic peak was calculated by integration, from which the heat associated with the dilution of $MBD1_{(1–75)}$ was subtracted for correction. These corrected heat values were normalized to the number of moles of injected $MBD1_{(1–75)}$ and are shown in Figure 6B. The titration curve was analyzed by nonlinear least-squares fitting to an appropriate binding model. The data were consistent with a simple 1:1 stoichiometry for $MBD1_{(1–75)}$−DNA complex formation. The dissociation constant, K_D, and the enthalpy change, ΔH, were obtained from the curve fitting and had values of $(47.5 \pm 8.7) \times 10^{-9}$ M and -13.5 ± 0.87 kcal/mol, respectively. The Gibbs free energy change, ΔG, and the entropy change, ΔS, were calculated using the equation

$$\Delta G = -RT\ \ln(1/K_D) = \Delta H - T\Delta S \quad (4)$$

The values obtained from these calculations are -9.94 ± 2.0 kcal/mol and -11.2 ± 2.0 cal $mol^{-1}\ K^{-1}$, respectively. Experimental errors were estimated from three independent measurements.

Table 1: Kinetic and Thermodynamic Parameters Obtained in This Work

	NMR	SPR	QCM	ITC
$k_{ex\ 25\ °C}$ (s^{-1})	4.30 ± 0.51	−	−	−
$k_{off\ 25\ °C}$ (s^{-1})	−	(3.26 ± 0.03) × 10^{-3}	(2.51 ± 0.38) × 10^{-3}	−
$k_{on\ 25\ °C}$ ($M^{-1}\ s^{-1}$)	−	(4.63 ± 0.17) × 10^{4}	(2.57 ± 0.39) × 10^{5}	−
K_D (nM)	−	70.4 ± 3.2	9.77 ± 2.96	47.5 ± 0.87

DISCUSSION

The kinetic and thermodynamic parameters obtained from this study are summarized in Table 1. To determine which of the two models, the flip model or the dissociation−reassociation model, is more appropriate for describing the chemical exchange phenomenon observed for the $MBD1_{(1–75)}$–methylated DNA complex, we compared k_{ex} and $1/(1/k_{on} + 1/k_{off})$. As k_{on} is much larger than k_{off} for the $MBD1_{(1–75)}$−DNA interaction, $1/(1/k_{on} + 1/k_{off})$ can be safely approximated to be equal to k_{off}. Therefore, if k_{ex} is on the same order of magnitude as k_{off}, the dissociation−reassociation model is more appropriate, where the reversal of the DNA strands relative to $MBD1_{(1–75)}$ is coupled with the total dissociation of DNA from $MBD1_{(1–75)}$. In contrast, if k_{ex} is much larger than k_{off}, the flip model is more appropriate, where the stochastic reversal of the DNA strands relative to $MBD1_{(1–75)}$ occurs without their complete dissociation. The dissociation rates, k_{off}, obtained from the results of SPR and QCM measurements are broadly consistent with each other and are in the range of 2–3.3 × 10^{-3} s^{-1} at 25 °C. These values are more than 3 orders of magnitude smaller than the exchange rate of the strands of the duplex DNA (k_{ex} = 4.30 ± 0.51 s^{-1} at 25 °C), which was estimated by chemical exchange 2D NMR spectroscopy. These results indicate that the flip model is more appropriate for explaining the strand exchange phenomenon. Despite the apparent limitation of the accuracy in the estimation of the k_{ex} value (Figure 3A), which seems to be mainly due to spin diffusion effects, the estimated k_{ex} values at variable temperatures fit reasonably well to the Arrhenius equation (Figure 3B), supporting the validity of the estimation.

It should be noted that the reported structure of the $MBD1_{(1–75)}$−methylated DNA complex indicates that the $MBD1_{(1–75)}$ in the complex is not able to invert its orientation with respect to the DNA without their dissociation, due to steric restriction, unless substantial structural change of the protein or DNA occurs. This observation leads us to hypothesize the existence of an alternative mode of binding of $MBD1_{(1–75)}$ to the methylated DNA, in which $MBD1_{(1–75)}$ undergoes a structural change that allows its rotation on the DNA. The key structural element in understanding this "soft binding mode" might be loop L1 of $MBD1_{(1–75)}$. In unliganded $MBD1_{(1–75)}$, this loop is highly mobile in solution as shown by the $^{1}H-^{15}N$ hetero-NOE (nuclear Overhauser effect) study and structure determination of unliganded $MBD1_{(1–75)}$ (*9*). Upon DNA binding, the loop seems to be induced to form a more rigid structure and latches onto the DNA backbone, contributing a substantial interfacial area to DNA. Consistent with this view, the average $^{1}H-^{15}N$ hetero-NOE value for residues in loop L1 in the complex was 0.74 ± 0.06, while that for the unliganded MBD was significantly smaller (0.32 ± 0.15) (*6*). The structure of the $MBD1_{(1–75)}$−methylated DNA complex suggests that this loop sterically restricts the rotational motion of $MBD1_{(1–75)}$. Therefore, it can be assumed that this intrinsically flexible loop might become unfolded at the hypothetical soft binding mode which allows the stochastic reversal of $MBD1_{(1–75)}$ with respect to the bound duplex DNA.

The soft binding mode of $MBD1_{(1–75)}$ may be relevant to the so-called nonspecific DNA binding mode (*15*). The nonspecific DNA binding mode of the *lac* repressor has been well illustrated by structure determination (*16*), showing that the protein bound to the DNA in a way distinctly different from that seen in the sequence-specific protein−DNA complex. The study also shows that an α helix is newly formed at the C-terminus of the protein upon switching from the nonspecific to specific binding mode, which is reminiscent of loop L1 of $MBD1_{(1–75)}$. It is therefore tempting to speculate that the hypothetical soft binding mode of $MBD1_{(1–75)}$ is closely related to the nonspecific binding mode. The nonspecific binding mode of $MBD1_{(1–75)}$ might be represented by its binding to nonmethylated DNA. SPR experiments showed that the dissociation constant, K_D, between $MBD1_{(1–75)}$ and nonmethylated DNA, the sequence of which is identical to that of the methylated DNA used in this study but lacking the cytosine methylation, was 5.63 ± 4.02 μM [determined by equilibrium binding measurement by SPR (data not shown)]. This value is approximately 100 times larger than that of the specific complex. Therefore, it may be possible that the conformation of $MBD1_{(1–75)}$ in the hypothetical soft binding complex may be related to that in the nonspecific complex.

In this study, flipping of an isolated MBD on the methyl-CpG DNA was examined. The question of whether the full-length MBD1 undergoes such a flipping motion under physiological conditions therefore arises. MBD1 is comprised of ~600 amino acid residues and has the N-terminal MBD, three cysteine-rich CXXC domains, and a C-terminal TRD (transcriptional repression domain). The activity of binding of the protein to the methylated DNA site seems solely defined by the MBD (*5*). Although CXXC domains are known to bind nonmethylated DNA, the action of MBD might be relatively independent of these due to the existence of a long linker region (~100 amino acid residues) separating these regions. Therefore, it is likely that, even in full-length MBD1, the MBD would be able to undergo a flipping motion on the methylated DNA just as the isolated MBD does. The molecular rotational correlation time (τ_c) of full-length MBD1 would be on the order of 10^{-7} s as estimated from its molecular weight. This is much shorter than the time scale of the chemical exchange (10^{-1} s as estimated from a k_{ex} of 4.3 s^{-1}). Thus, the slower tumbling of full-length MBD1 compared to that of the isolated MBD seems largely to not affect the flipping motion. In the cells, MBD1 may exist as a large complex with other transcriptional regulators. However, even for a megadalton complex, τ_c would be estimated still to be on the order of 10^{-6} s, suggesting that such a complex would be capable of tumbling in solution faster than

the flipping motion observed for the isolated MBD. Thus, taking into consideration the rate of tumbling, it is likely that full-length MBD1 might be able to undergo flipping at the methyl-DNA site. However, it is possible that interactions of the CXXC domains of MBD1 and other regions in the protein complex with DNA modulate the motion.

What is then the biological significance of the flip motion of MBD1? The functions of MBD family proteins include recruitment of a variety of chromatin remodeling complexes that contain HDAC (histone deacetylase), HMT (histone methyltransferase), MCAF1 (MBD1-containing chromatin-associated factor-1), or others to methylated sites on genomic DNA (*17–21*). Thus, the MBD protein exists as a component of large protein complexes rather than as an isolated monomeric protein when they bind to methylated DNA in the nucleus. These chromatin remodeling complexes are thought to enzymatically modify and/or remodel histones of chromatins that are located at or near the methylation sites. To exert their effects over large areas around the methylation sites, the ability of the complexes to reverse the orientation at the methylated sites may be beneficial as it provides more degrees of freedom to the molecule. Alternatively, when the complex contains another DNA binding subunit, the reversibility of the MBD at the methylation site may facilitate the binding of this subunit to its target site on DNA, depending on the relative positions of this and the methylation sites on DNA. Moreover, this rotational motion may somewhat reduce the entropy cost associated with complex formation and thereby contribute to the affinity of MBD for the methylated DNA to some extent.

In conclusion, by employing ^{13}C-filtered ^{1}H−^{1}H 2D NOESY combined with other analytical methods, such as SPR, ITC, and QCM, we present data that show the MBD of MBD1 reverses its orientation relative to the methylated DNA without complete dissociation from DNA. To the best of our knowledge, this is the first experimental evidence that a protein undergoes a flip motion at a protein−DNA interface and may lead us to a better understanding of the roles of the MBD in chromosomal remodeling as well as in the general biophysical properties of protein−DNA interactions.

ACKNOWLEDGMENT

We thank Dr. K. Morikawa for his help in recording ITC data.

REFERENCES

1. Costello, J. F., and Plass, C. (2001) Methylation matters. *J. Med. Genet. 38*, 285–303.
2. Bird, A. P., and Wolffe, A. P. (1999) Methylation-induced repression: Belts, braces, and chromatin. *Cell 99*, 451–454.
3. Robertson, K. D., and Wolffe, A. P. (2000) DNA methylation in health and disease. *Nat. Rev. Genet. 1*, 11–19.
4. Jones, P. A., and Takai, D. (2001) The role of DNA methylation in mammalian epigenetics. *Science 293*, 1068–1070.
5. Hendrich, B., and Bird, A. (1998) Identification and characterization of a family of mammalian methyl-CpG binding proteins. *Mol. Cell. Biol. 18*, 6538–6547.
6. Ohki, I., Shimotake, N., Fujita, N., Jee, J., Ikegami, T., Nakao, M., and Shirakawa, M. (2001) Solution structure of the methyl-CpG binding domain of human MBD1 in complex with methylated DNA. *Cell 105*, 487–497.
7. Ballestar, E., and Wolffe, A. P. (2001) Methyl-CpG-binding proteins: Targeting specific gene repression. *Eur. J. Biochem. 268*, 1–6.
8. Katoh, E., Yamazaki, T., Kiso, Y., Wingfield, P. T., Stahl, S. J., Kaufman, J. D., and Torchia, D. A. (1999) Determination of the rate of monomer interchange in a ligand-bound homodimeric protein from NOESY cross peaks: Application to the HIV protease/KNI-529 complex. *J. Am. Chem. Soc. 121*, 2607–2608.
9. Ohki, I., Shimotake, N., Fujita, N., Nakao, M., and Shirakawa, M. (1999) Solution structure of the methyl-CpG-binding domain of the methylation-dependent transcriptional repressor MBD1. *EMBO J. 18*, 6653–6661.
10. Zwahlen, C., Legault, P., Vincent, S. J. F., Greenblatt, J., Konrat, R., and Kay, L. E. (1997) Methods for measurement of intermolecular NOEs by multinuclear NMR spectroscopy: Application to a bacteriophage λ N-peptide/boxB RNA complex. *J. Am. Chem. Soc. 119*, 6711–6721.
11. Delaglio, F., Grzesiek, S., Vuister, G. W., Zhu, G., Pfeifer, J., and Bax, A. (1995) NMRPipe: A multidimensional spectral processing system based on UNIX pipes. *J. Biomol. NMR 6*, 277–293.
12. Goddard, T. D., and Kneller, D. G. (1999) SPARKY 3; University of California: San Francisco.
13. Matsuno, H., Niikura, K., and Okahata, Y. (2001) Design and characterization of asparagine- and lysine-containing alanine-based helical peptides that bind selectively to A.T base pairs of oligonucleotides immobilized on a 27 MHz quartz crystal microbalance. *Biochemistry 40*, 3615–3622.
14. Okahata, Y., Niikura, K., Sugiura, Y., Sawada, M., and Morii, T. (1998) Kinetic studies of sequence-specific binding of GCN4-bZIP peptides to DNA strands immobilized on a 27-MHz quartz-crystal microbalance. *Biochemistry 37*, 5666–5672.
15. Halford, S. E., and Marko, J. F. (2004) How do site-specific DNA-binding proteins find their targets? *Nucleic Acids Res. 32*, 3040–3052.
16. Kalodimos, C. G., Biris, N., Bonvin, A. M. J. J., Levandoski, M. M., Guennuegues, M., Boelens, R., and Kaptein, R. (2004) Structure and flexibility adaptation in nonspecific and specific protein-DNA complexes. *Science 305*, 386–389.
17. Ng, H. H., Zhang, Y., Hendrich, B., Johnson, C. A., Turner, B. M., Erdjument-Bromage, H., Tempst, P., Reinberg, D., and Bird, A. (1999) MBD2 is a transcriptional repressor belonging to the MeCP1 histone deacetylase complex. *Nat. Genet. 23*, 58–61.
18. Wade, P. A., Gegonne, A., Jones, P. L., Ballestar, E., Aubry, F., and Wolffe, A. P. (1999) Mi-2 complex couples DNA methylation to chromatin remodelling and histone deacetylation. *Nat. Genet. 23*, 62–66.
19. Bird, A. (2002) DNA methylation patterns and epigenetic memory. *Genes Dev. 16*, 6–21.
20. Fujita, N., Watanabe, S., Ichimura, T., Tsuruzoe, S., Shinkai, Y., Tachibana, M., Chiba, T., and Nakao, M. (2003) Methyl-CpG binding domain 1 (MBD1) interacts with the Suv39h1-HP1 heterochromatic complex for DNA methylation-based transcriptional repression. *J. Biol. Chem. 278*, 24132–24138.
21. Sarraf, S. A., and Stancheva, I. (2004) Methyl-CpG binding protein MBD1 couples histone H3 methylation at lysine 9 by SETDB1 to DNA replication and chromatin assembly. *Mol. Cell 15*, 595–605.

BI7019029